Breast Image Registration Using Non-Linear Local Affine Transformation

Feiyu Chen[a], Peng Zheng[a], Penglong Xu[a], Andrew D. A. Maidment[b], Predrag R. Bakic[b], David D. Pokrajac[a], Fengshan Liu[a], Xiquan Shi[a]

[a]Delaware State University, 1200 N DuPont Hwy, Dover DE 19904;
[b]University of Pennsylvania, 3400 Spruce Street, Philadelphia, PA 19104

ABSTRACT

A novel breast image registration method is proposed to obtain a composite mammogram from several images with partial breast coverage, for the purpose of accurate breast density estimation. The breast percent density estimated as a fractional area occupied by fibroglandular tissue has been shown to be correlated with breast cancer risk. Some mammograms, however, do not cover the whole breast area, which makes the interpretation of breast density estimates ambiguous. One solution is to register and merge mammograms, yielding complete breast coverage. Due to elastic properties of breast tissue and differences in breast positioning and deformation during the acquisition of individual mammograms, the use of linear transformations does not seem appropriate for mammogram registration. Non-linear transformations are limited by the changes in the mammographic projections pixel intensity with different positions of the focal spot. We propose a novel method based upon non-linear local affine transformations. Initially, pairs of feature points are manually selected and used to compute the best fit affine transformation in their small neighborhood. Finally, Shepherd interpolation is employed to compute affine transformations for the rest of the image area. The pixel values in the composite image are assigned using bilinear interpolation. Preliminary results with clinical images show a good match of breast boundaries, providing an increased coverage of breast tissue. The proposed transformation can be controlled locally. Moreover, the method is converging to the ground truth deformation if the paired feature points are evenly distributed and its number is large enough.

Keywords: Digital mammography, image registration, affine transformation, Shepherd interpolation.

1. INTRODUCTION

Breast density, the relative amount of fat and dense tissue in the breast as seen in a mammogram, has been shown to be correlated with breast cancer risk. A number of methods[1][2] have been proposed to measure breast density from mammograms. However, some mammograms do not cover the entire patient's breast, e.g., due to large breast size in comparison to the x-ray imaging detector. This is of particular importance for the estimation of breast density, a biomarker of breast cancer risk. Partial breast visualization limits our ability to calculate breast density. One solution is to register and merge such partial mammograms, yielding complete breast coverage. Registration of mammograms is challenging because the mammogram is a 2D projection of non-rigid breast tissues. As a result, the 3D arrangement of the breast tissue is not exactly replicated in partial projections of large breasts. This is further complicated by differences in mammographic compression between images.

Registration techniques can be categorized as: 1) feature based techniques[3][4], which use feature points to match the images; 2) intensity based algorithms[5], which use the gray value of images; and 3) hybrid methods[6] that generate mapping between images (using feature points) with constraint on their intensity. For all of these registration techniques, a transformation must be determined so that the points in warped image can be related to their corresponding points in the reference image. Based on the number of degrees of freedom, the transformation models can use linear transformation (rigid and affine), elastic models or diffeomorphic transformations. Local controls cannot be achieved from the linear transformation model as the global parameters are computed for the entire image. The elastic model offer high order control, but the performance of elastic models is a balance between flexibility and computational complexity. Diffeomorphic transformations, which preserve topology, have resulted in good performance in a number of applications including brain MRI image registration.

The main difficulty of feature-based methods is to extract and match intrinsic feature points from mammograms, as there are no significant landmarks in a mammogram except the nipple. In this paper, a novel feature based approach, non-linear local affine transformation, is proposed to obtain a composite image from several images with partial breast coverage. Feature points are manually selected near the nipple, breast boundary and inside the

Medical Imaging 2013: Physics of Medical Imaging, edited by Robert M. Nishikawa, Bruce R. Whiting, Christoph Hoeschen,
Proc. of SPIE Vol. 8668, 86684J · © 2013 SPIE · CCC code: 1605-7422/13/$18 · doi: 10.1117/12.2008033

breast based upon visual similarity in both mammograms. Affine transformations between sets of feature points are then computed. Finally, Shepherd interpolation [7] is used to extend affine transformations to the entire breast. The pixel values in the composite image are assigned using the average of different images. Results with clinical images show that the resulting image cover different parts of original images, and the same texture from both registered images has a good agreement in composite image.

Qualitative testing is presented on selected images from the ACRIN DMIST database[8]. This work was tested with anonymized images obtained about IRB ethical review. A clinical image was split into two overlapping partial images; one partial image was transformed (the warped image), while another was not modified (the reference image). Those images were treated as a pair of mammograms with different coverage.

2. METHODOLOGY

2.1 Extraction of feature points

Our algorithm requires that feature points be extracted prior to registration, and the result of registration will depend on the reliability and accuracy of the extracted features. Automatic identification and extraction of feature points is difficult due to the non-linear compression deformation and the lack of significant landmarks in mammograms (Fig. 1). Typically, the features are the center of ROI, crossing points, end points and middle points. We observe the prominent features (such as ducts and blood vessels) from both images, Fig. 1. The crossing points are determined upon visual similarity in both mammograms. Due to compression and different positions of the breast, the coordinates of those crossing points may be different in the two mammograms, but the orientation of feature and local curvature of crossing points are more likely to be preserved. The advantage of our manual extraction is that the correspondence of two sets of feature points can be established during the extraction step. We also select other features (end points and middle points) in a small neighborhood around the selected crossing points. Subsequently, the deformation between two sets of feature points can be estimated.

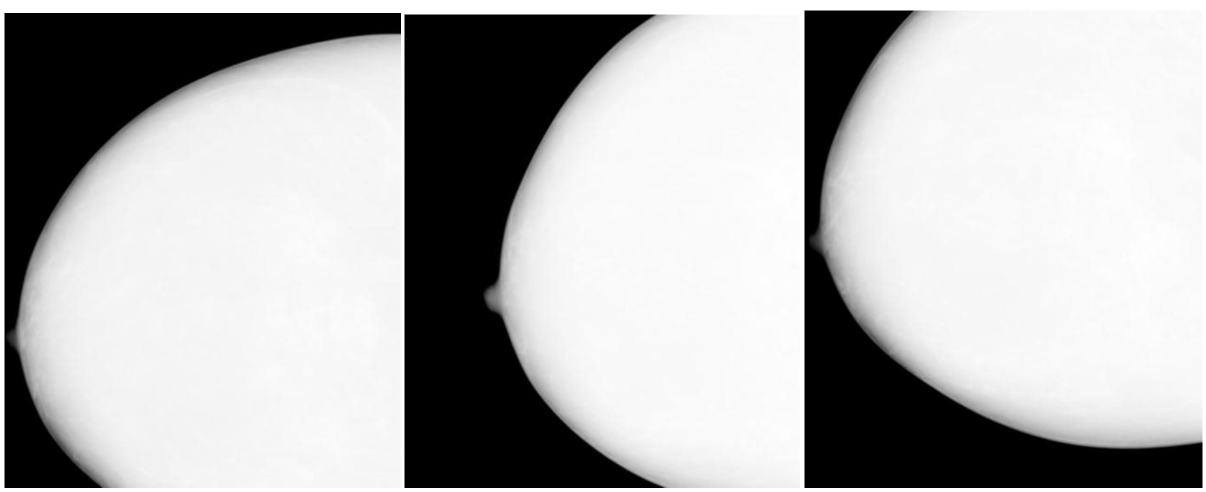

Figure 1: Three clinical images of the same patient from ACRIN DMIST database demonstrating partial breast coverage.

2.2 Best affine transformation

Given two sets of feature points in two images that need to be registered, we assume the deformation between them can be approximated by affine transformation, which can be considered as a first-order approximation of the true transformation resulting from breast projection.

We denote the two images obtained from different angle and different compression by I_1 and I_2, and assume $S_1 = \{X_1, X_2, \cdots, X_n\}$ be a set of feature points in I_1 (reference image), and $T_1 = \{Y_1, Y_2, \cdots, Y_n\}$ be the corresponding set in I_2 (warped image). Particularly, X_1 and Y_1 are the crossing points in each set, called the centers of S_1 and T_1. The affine transformation $\varphi : \varphi(x) = Ax + b$ mapping S_1 into T_1 can be obtained by solving the optimization problem:

$$\underset{A\in R^2\times R^2, b\in R^2}{\arg\min} \sum_{j=1}^{n} \left\| AX_j + b - Y_j \right\|^2 \qquad (1)$$

where A is a 2x2 matrix including scaling and rotation, $b \in R^2$ is a translation vector.

The solution of the above optimization problem can be expressed as:

$$[A,b] = \left([Y]_{2\times n} \begin{bmatrix} X \\ 1 \end{bmatrix}^T_{n\times 3} \right)_{2\times 3} \left(\begin{bmatrix} X \\ 1 \end{bmatrix}_{3\times n} \begin{bmatrix} X \\ 1 \end{bmatrix}^T_{n\times 3} \right)^{-1}_{3\times 3} \qquad (2)$$

where $X = \left[X_1, X_2, \cdots, X_n \right]$ and $Y = \left[Y_1, Y_2, \cdots, Y_n \right]$.

Similarly, for each corresponding pairs of feature sets $(S_1,T_1),(S_2,T_2),\cdots,(S_k,T_k)$, we can also obtain the best affine transformations $\varphi_1,\varphi_2,\cdots,\varphi_k$ that minimize the least square error. Note that if we consider $\{\varphi_i\}$ as a basis, then for an arbitrary point in I_1, we can find its affine transformation by combining the basis with different non-linear weights [see equation (3) below].

2.3 Non-linear Local Affine Transformation

The Shepard interpolation [7], which is a simple case of inverse distance weighting to assign value to unknown points based on given points, is employed to compute the local affine transformation φ for each non-feature point in the image.

Assume X_i and Y_i are the centers of S_i and T_i, i.e., the affine transformation of X_i is φ_i, obtained from equation (2). For any other point Z in I_1, its corresponding local non-linear affine transformation φ is defined as:

$$\varphi(Z) = \begin{cases} \dfrac{\sum_{i=1}^{k} d_i^{-\alpha} \varphi_i}{\sum_{i=1}^{k} d_i^{-\alpha}} & \text{if } (\forall i)\, Z \neq X_i \\ \varphi_i & \text{if } (\exists i)\, Z = X_i \end{cases} \qquad (3)$$

where $d_i = \left| X_i - Z \right|$ is the Euclidean distance between X_i and Z. Note that non-linear deformation mapping φ is continuous since $\lim_{Z\to X_i} \varphi(Z) = \varphi_i$. Moreover, the partial derivatives with respect to two coordinates of φ exist at all the points if $\alpha > 1$. We choose the default value of α as 2 for convenience of computation. The function $\varphi(Z)$ can be considered as the first order approximation of the ground truth deformation in a small neighbor of Z. It will converge to the ground truth deformation when the number of neighbors k is large enough and the feature points are evenly distributed. Note also that φ can be expressed locally as a linear combination of affine transformations. Moreover, local controls can be achieved if we add or delete feature sets in the region of interest.

The purpose of our image registration is mapping both I_1 and I_2 into same region to get composite image, say I_c. I_1 can be mapped to I_c by a translation transformation; while the non linear local affine transformation φ was used to estimate the mapping between I_2 and I_c, which will change the shape of image I_c.

In order to initialize the size of I_c, we have to determine the maximum and minimum value of I_2 under the local affine transformation $\varphi(x)$, where x can be represented by linear combination of four corner points c_j of I_2.

$$x = \sum_{j=1}^{4} w_j c_j \qquad \varphi(x) = \varphi\Big(\sum_{j=1}^{4} w_j c_j\Big) = \sum_{j=1}^{4} w_j \varphi(c_j). \qquad (4)$$

According to equation (3), we know that $\varphi(x)$, the local affine transformation at point x, is the linear average of φ_i with weight 1, therefore:

$$\max_x \varphi(x) = \max_i(\max_j \varphi_i(c_j)), \quad \min_x \varphi(x) = \min_i(\min_j \varphi_i(c_j)). \qquad (5)$$

Now we can classify I_c into four different regions R_1: the points x that have only inverse image y in I_1; R_2: the points x with inverse image z only from I_2; R_3: the points x that have inverse images y both in I_1 and in I_2; R_4:

the points that do not have any inverse image. The following strategy is used to assign gray values to the points in I_c.

$$I_c(x) = \begin{cases} I_1(y) & x \in R_1 \\ I_2(z) & x \in R_2 \\ \dfrac{I_1(y)+I_2(z)}{2} & x \in R_3 \\ 0 & x \in R_4 \end{cases} \quad . \tag{6}$$

2.4 Image validation method

The simplest validation is obtained from examination of the pixel-wise brightness difference between the reference image and the transformed warped image. However, such technique does not provide good performance for mammogram registration due to the 3D various projections of the breast tissues. Even if the positions of the image features are matched in the warped image and the reference image, the pixel brightness of same features will be different since the path of X-ray is different.

As an initial validation, individual clinical images were transformed to mimic partial coverage as illustrated in Fig. 2. A clinical image is split into two overlapping partial images. One partial image was transformed (the warped image) and another was not modified (the reference image). Those images were treated as a pair of mammograms with different coverage. The registration error can be computed as the difference between the original image and the composite image after the registration.

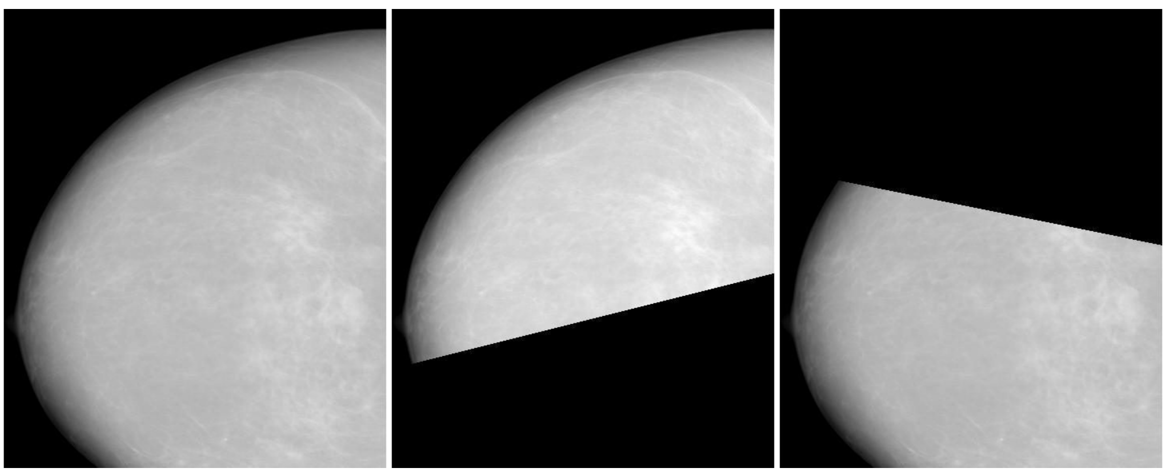

Figure 2: Original image and partial images (1 and 2) for validation.

3. RESULTS

In this section we present preliminary results using the proposed approach applied to clinic mammograms taken from the ACRIN DMIST database of mammograms. This work is a part of a larger study of racial disparity in breast cancer risk. For that project, breast percent density and parenchymal texture of minority women and age-matched Caucasian controls from the ACRIN DMIST database[8] are being compared.

Fig. 3 (a,b) illustrates the registration of two images from a large breast using the proposed non-linear local affine transformation with 9 pairs of feature sets. The effect of the choice of reference image is shown. Fig. 3c shows the composition of 3 partial views that covers the whole breast.

Fig. 4 illustrates the qualitative comparison of the proposed method with the result of Advanced Normalization Tools[9], (ANTs) that computes the unsupervised optimal diffeomorphic transformation by minimizing the similarity measure between warped image and reference image. The registered image of the warped image (Fig. 4a) and reference image (Fig. 4b) is shown in Fig. 4c. Fig. 4c illustrates the result of ANTs.

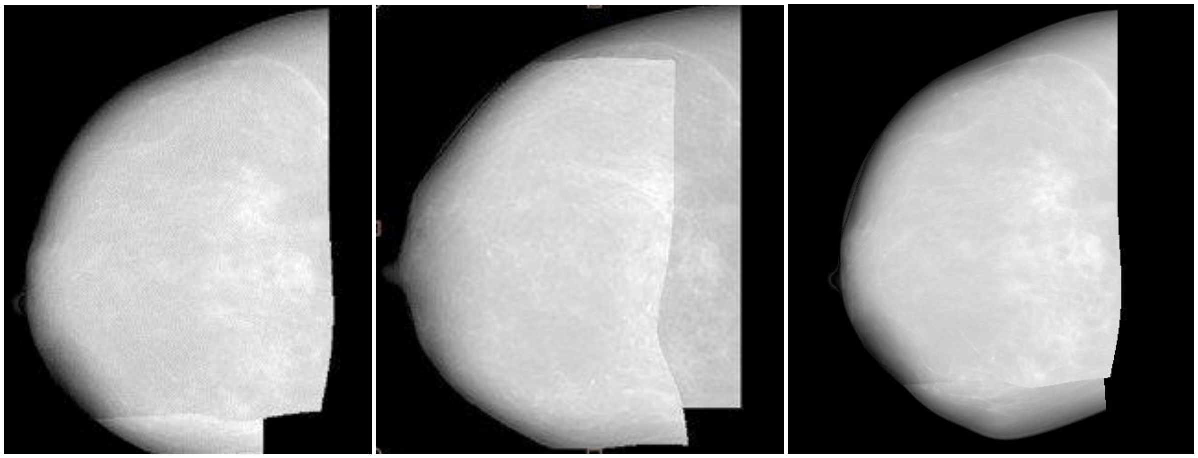

Figure 3a, b: Two partial images combined following registration, showing the effect of the choice of reference image. Figure 3c: The same breast showing the composition of three images in figure 1 after logarithm of grayscale values.

Fig. 5 illustrates the comparison of the original and the registered image. The reference (Fig. 5a) and the warped image (Fig. 5b) are obtained from Fig.2c. Fig. 5c illustrates the registered image using the proposed method, and Fig. 5d shows the difference between the composite and the original image (Fig. 1a after taking the logarithm).

4. DISCUSSION

To date, we have been able to achieve anecdotal results that support continued development and testing of this new method. Fig. 3 (a,b) suggests that the proposed method is robust, since the results of registration are similar regardless of the choice of the reference image (comparing Figs. 3a and 3b. Fig. 3 indicates that the observable features, especially the nipple and the boundary of skin, have good agreement.

Fig. 4 suggusts that the results of the proposed method are comparable to the results of the diffeomorphic transform implemented using ANTs, an open source software package. Particularly, the textures of warped image are preserved in registered images, and the shape of registered image is similar as reference image. The proposed method may have difficulties in registering some regions of the image (corresponding to region R_4, see equation (6)). Fig. 5 suggests that the features in the composite image show good agreement. The registration error is smaller in the region of overlap (the upper part of the registered image), since we can extract the corresponding feature points only from this region.

In our future work, we will apply the technique to more images in the DMIST database and develop statistical measures of the registration accuracy.

5. CONCLUSIONS

A novel registration task is proposed, and two methods are compared in this task. This study indicates that our newly proposed method may provide fast and comparatively accurate registration of overlapping breast images. The method may be of value whether used standalone or for initialization of other modern registration techniques (e.g., diffeomorphic transformation). The major drawback of the proposed method is the need for manual extraction of feature points. Further work is needed on application of automatic feature selection (e.g., SIFT algorithm [10]). Finally, we plan to perform more extensive quantitative validation of the proposed algorithm on a series reference and warped images extracted from all the applicable images in the ACRIN database.

6. ACKNOWLEDGMENT

This work was supported in part by the US Department of Defense (Breast Cancer Research Program HBCU Partnership Training Award #BC083639 and the Center for Advanced Algorithms grant and Adaptive Approach to Identify Unusual Behavior in Video Imagery grant #54412-CI-ISP) and the US National Science Foundation (CREST grant #HRD-1242067).

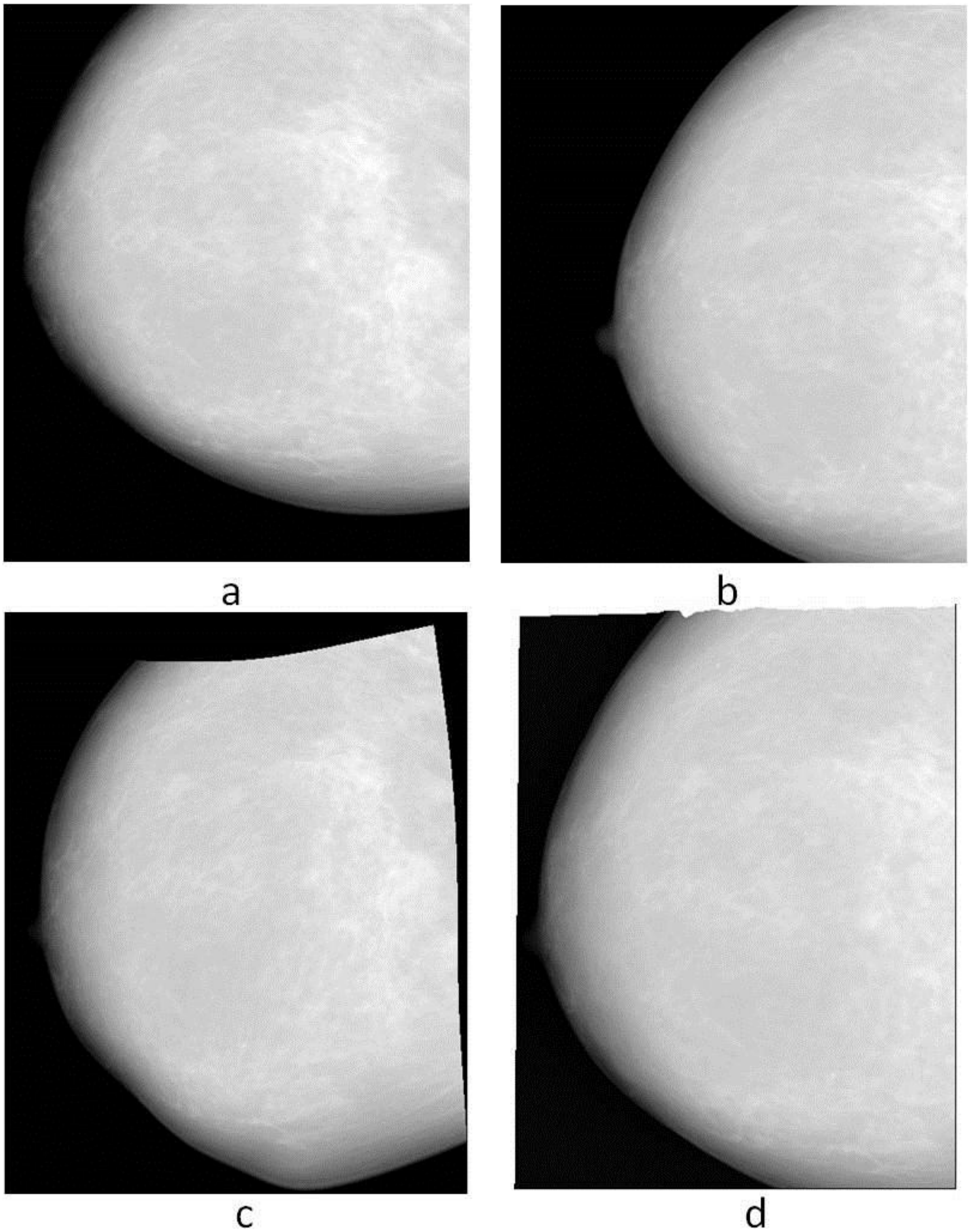

Figure 4: Warped image (a), reference image (b) and the result using the proposed method (c) and Advanced Normalization Tools (ANTs)[9] (d).

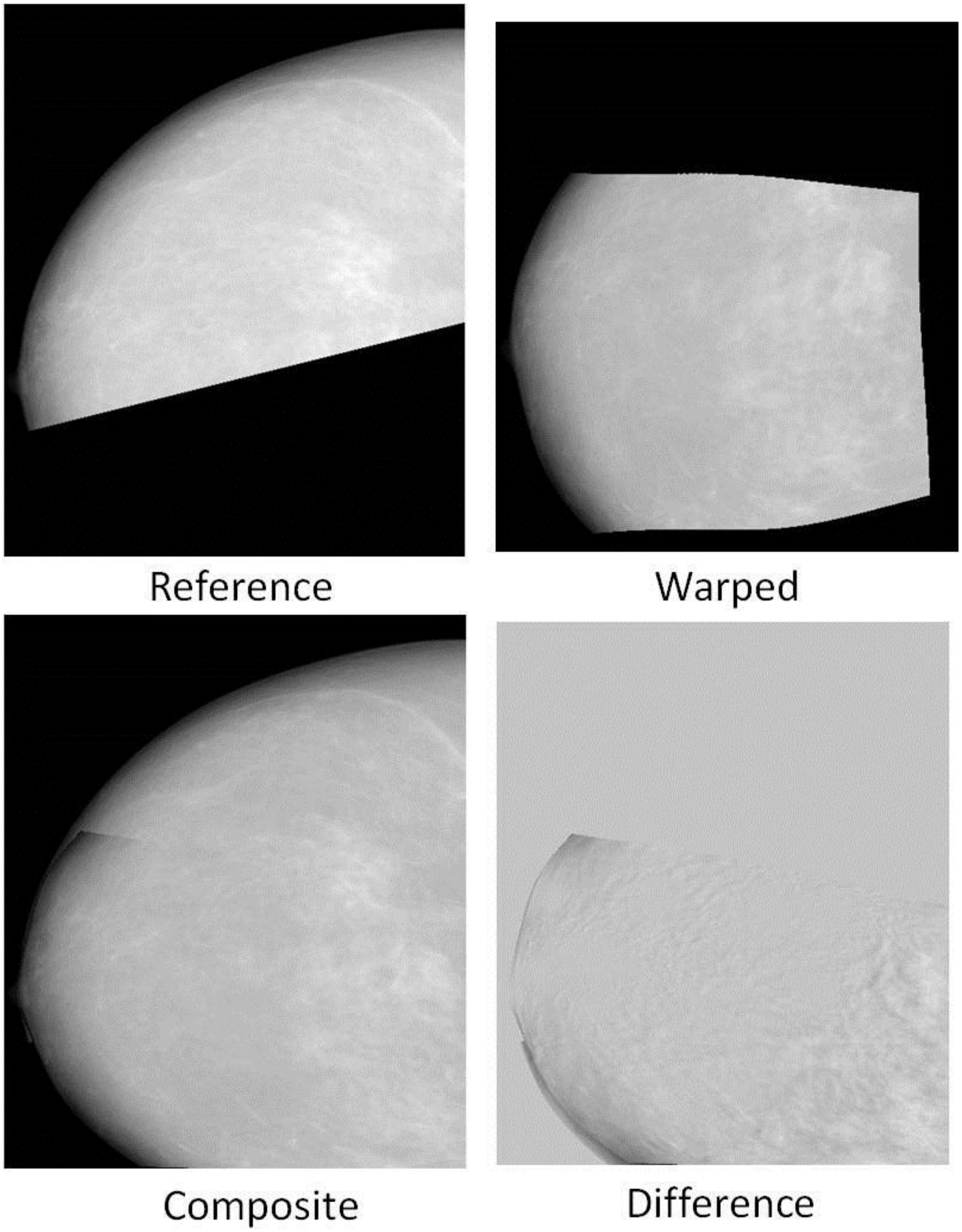

Figure 5: Example validation.

REFERENCES

1. McCormack VA, Highnam R, Perry N, dos Santos Silva I. Comparison of a new and existing method of mammographic density measurement: intramethod reliability and associations with known risk factors. *Cancer Epidemiol Biomarkers Prev. 16*, 1148–1154 (2007)

2. Kontos D, Bakic PR, Acciavatti RJ, Conant EF, Maidment ADA. A Comparative study of volumetric and area-based breast density estimation in digital mammography: result from a screening population. *Digital Mammography*. LNCS 6136:378–385.

3. Petroudi S, Brady M. Textons contours and regions for improved mammogram registration digital mammography. IWDM 2004, June 2004, Springer, Chapel Hill.

4. Marti R, Zwiggelaar R, Rubin CME. Automatic mammographic registration: towards the detection of abnormalities. Detection of linear structures in mammographic images. *Medical image understanding analysis.* (2001)

5. Brzakovic D, Vujovic N, Neskovicand M, Brzakovic P, Fogerty K (1996) Mammogram analysis by comparison with previous screenings. In: Doi K, Giger ML, Nishikawa RM, Schmidt RA (eds) Digital Mammogrphy' 96, Elsevier, Amsterdam

6. Wirth MA, Narhan J, Gray D (2002) Nonrigid mammogram registration using mutual information. Proc SPIE 4684:562 – 573.

7. Shepard, D. (1968) A two-dimensional interpolation function for irregularly-spaced data, Proc. 23rd National Conference ACM, ACM, 517-524.

8. Pisano ED, Gatsonis C, Hendrick E, et al. Diagnostic Performance of Digital versus Film Mammography for Breast-Cancer Screening. NEJM 2005; 353:1773-1783.

9. Avants BB, Tustison, N.J., Song, G., Gee, J.C., 2009. ANTS: Advanced Open-Source Normalization Tools for Neuroanatomy. Penn Image Computing and Science Laboratory.

10. Lowe DG, Object recognition from local scale-invariant features. *Proceedings of the International Conference on Computer Vision*. 2. pp. 1150–1157.